Eur Biophys J (2005) 34: 67–81
DOI 10.1007/s00249-004-0425-0

ARTICLE

Giordano M. Di Gregorio · Paolo Mariani

Rigidity and spontaneous curvature of lipidic monolayers in the presence of trehalose: a measurement in the DOPE inverted hexagonal phase

Received: 4 November 2003 / Revised: 26 January 2004 / Accepted: 18 May 2004 / Published online: 30 September 2004

Abstract Trehalose is a sugar which plays an important protectant role in organisms against damage due to dehydration. To explore the basic molecular mechanism which governs the protective function exerted on lipid membranes, X-ray diffraction and osmotic stress experiments have been performed on L-α-dioleoyl-phosphatidyl-ethanolamine (DOPE) in trehalose solutions of different concentrations. In pure water, DOPE forms an inverted hexagonal (H_{II}) phase; in sugar solutions, a strong dehydration, which induces a large reduction of the H_{II} lattice parameter, has been detected, but nevertheless no phase transitions occur. Structural data, directly obtained from reconstructed electron density maps, show that the bending of the lipid monolayer induced by the sugar is coupled to changes in the DOPE molecular shape. By osmotic stress, the work required to dehydrate the monolayer has been obtained and the overall free energy described as a function of trehalose concentration. Three results should be stressed: (1) dehydration experiments performed in the presence of sugar demonstrate that the protective effect cannot be purely osmotic; (2) the pivotal surface, that location on the molecule whose area is invariant upon isothermal bending, has been analyzed by two different methods: the approach by Rand and co-workers and the approach by Templer and co-workers; in both cases its presence along the DOPE molecule has been revealed and its position estimated; (3) the spontaneous radius of curvature and the rigidity constant of the lipid monolayer, measured at the pivotal plane, changes from 3.06 nm (in pure water) to 2.82 nm (in 1.4 M trehalose), and from 0.55×10^{-19} to 0.74×10^{-19} J, respectively. We assume that these modifications are related to direct interactions between trehalose and DOPE that alter the interface geometry, reducing the repulsion between the polar heads. However, the increased bending rigidity also accounts for the changes of the property of the aqueous compartment, reflecting the rigidity and stiffness of the sugar matrix around and inside the lipid phase.

Keywords Hydration · Lipid model membrane · Osmotic stress · Trehalose function · X-ray diffraction

G. M. Di Gregorio · P. Mariani (✉)
Dipartimento di Scienze Applicate ai Sistemi Complessi,
Università Politecnica delle Marche and INFM,
via Ranieri 65, 60131 Ancona, Italy
E-mail: mariani@alisf1.univpm.it
Tel.: +39-071-2204608
Fax: +39-071-2204605

Introduction

Trehalose is a disaccharide which exerts a unique protective function on many organisms against damage due to dryness (Crowe et al. 1984; Crowe and Crowe 1988; Takahashi et al. 1997; Crowe 2002). Several plant seeds, spores and macrocysts, as well as some species of soil-dwelling animals, have in fact been observed to survive to complete dehydration for several years in a state of suspended animation (anhydrobiosis), while they rapidly swell and resume their metabolic functions upon re-hydration. A common theme for all these organisms is that they contain large amounts of two disaccharides, trehalose or sucrose, in the dry state. Therefore, the nature of the protective effect was unclear, but survival was correlated with the intracellular synthesis of trehalose during desiccation, and with its degradation after re-hydration (Crowe 2002).

Several mechanisms have been considered to explain how trehalose could effect survival. In the anhydrous state, sugar molecules have been described to substitute water molecules by hydrogen bonding the hydrophilic surfaces of proteins or lipids (Crowe et al. 1987; Crowe and Crowe 1988; Crowe 2002). In particular, the formation of hydrogen bonds between the phospholipid phosphate and the sugar hydroxyls has been demonstrated by infrared spectroscopy (Crowe et al. 1984) and the lowering of the phase transition temperatures

detected in these conditions has been suggested to derive from the spreading apart of the phospholipid headgroups, which decreases the van der Waals interactions between the acyl chains (Crowe 2002). Considering that an amorphous solid (a glass) forms by drying a trehalose solution, it has been also proposed that is the physical state of the sugar matrix which plays a major role in the protective function (Cordone et al. 1998; Crowe 2002; Librizzi et al. 2002). The glass formation can in fact account for the prevention of protein denaturation and cell fusion, since both phenomena involve intra- and intermolecular motions which are hindered in the glassy state. Moreover, the rigidity of the sugar matrix rather than a direct lipid–sugar interaction has been invoked to explain the temperature depression of the L_β-to-L_α lamellar phase transition detected in sucrose glasses (Zhang and Steponkus 1996; Shalaev and Steponkus 2001). Analogous hindering has also been reported for carboxy-myoglobin embedded in a trehalose matrix by Rector et al. (2001) and by Librizzi et al. (2002). Both groups of authors suggested that structural fluctuations, involving the displacement of protein surface, can take place even in highly viscous fluids, but are severely hindered when the surface topology is fixed by a solid glass.

In fully hydrated systems, the protective mechanism has been described differently. Like other large hydrophilic molecules, trehalose can be preferentially solubilized within the bulk of the solution and be excluded from the solvation layers of the macromolecular surfaces. This leads to the dehydration of such surfaces (and, in turn, to the reduction of the interfacial area), which become less flexible and therefore more thermally stable (Koynova et al. 1989). Under these conditions, molecular dynamic simulations on the carboxy-myoglobin molecule embedded in a 50% (w/w) trehalose solution (Cottone et al. 2002) showed that the protein is mostly surrounded by water, and only a few trehalose molecules are bound to the protein through only one OH group.

Lipid dehydration experiments performed in the presence of sugars demonstrated, on the contrary, that the protective effect cannot be purely osmotic. In the monoolein–water system, where several inverse phases exist as a function of concentration (Mariani et al. 1988), no phase transitions occur when dehydration is performed in the presence of trehalose, even when extremely dry conditions are reached (Mariani et al. 1999; Saturni et al. 2001). Analogously, in the case of the dioleoyl-phosphatidyl-ethanolamine, it has been observed that sucrose prevents the formation of the ordered and partially ordered phases occurring at moderate and low hydration, such as the L_α phase (Shalaev and Steponkus 2001; Rappolt et al. 2003). All these observations clearly suggest that the sugar effect should be related to an additional stabilization of the lipid monolayer exerted by the sugar during dehydration.

Under this viewpoint, the kosmotropic properties of trehalose must be considered (Collins and Washabaugh 1985). This sugar has been definitely classified as a net water-structurer (Koynova et al. 1997); in particular, it interferes with the tetrahedral network of water, structuring out to the third solvation layer, in such a way to reduce the amount of freezable water (Branca et al. 2002). As a consequence, trehalose solutions tend to minimize the area-per-molecule at the lipid/water interface, stabilizing structures with low surface areas (like inverted cubic or hexagonal phases), or inducing transitions from structures with larger to structures with lower interfacial area (Wistrom et al. 1989; Mariani et al. 1999; Saturni et al. 2001; see also references in Crowe 2002).

To resolve the different aspects related to the mechanism of interaction between sugars and lipid layers, we resort to the structural analysis of a lipid system which forms an inverse non-lamellar phase in excess of water (see Mariani et al. 1999; Saturni et al. 2001). It should be noted that in order to analyze the effects of external molecules (both water- or lipid-soluble) on lipid systems, such an approach is rather common. We note that with this approach it is relatively easy to derive a number of mechanical parameters such as the monolayer intrinsic curvature, the monolayer resistance to the bending or stretching, the location of the pivotal or neutral surface and so on. These parameters in turn describe the stability and the energetics of the various mesophases, including of course the properties of the biologically most relevant lamellar L_α phase (see, for example, Gawrish et al. 1992; Kozlov et al. 1994; Leikin et al. 1996; Koynova et al. 1997; Chen and Rand 1998; Fuller and Rand 2001; Harper et al. 2001; Shalaev and Steponkus 2001; Rappolt et al. 2003; Szule and Rand 2003).

In this work, we analyzed by X-ray diffraction experiments performed under osmotic stress the dehydration behavior and the structural properties of dioleoyl-phosphatidyl-ethanolamine (DOPE) in trehalose solutions. While the phase characteristics of DOPE at different hydration levels are well known (Rand et al. 1990; Gawrish et al. 1992; Rand and Fuller 1994; Leikin et al. 1996; Chen and Rand 1998; Fuller and Rand 2001; Szule and Rand 2003), the sugar effects on DOPE have been considered only in excess water conditions. As a main result, Wistrom and co-workers (1989) and Koynova and co-workers (1997) showed that in excess of trehalose solutions the H_{II} phase forms directly from the gel L_β phase, without the intervening lamellar liquid-crystalline L_α phase.

Materials and methods

L-α-Dioleoyl-phosphatidyl-ethanolamine (DOPE) (99% purity), high-molecular-weight polyethylene glycol (PEG 8,000 MW and PEG 20,000 MW) (99% purity), dextran and D-trehalose dihydrate (95% purity) were obtained from Sigma-Aldrich and used without further purification. To prepare lipid mixtures in excess of sugar

solutions, DOPE was first dissolved in chloroform and dried under vacuum (Rand et al. 1990). The powder was then hydrated in 2 mM TES buffer excess solution (pH 7.3) over a range of trehalose concentrations. Finally, the samples were equilibrated at least for 24 h at 25 °C before X-ray diffraction analysis.

The osmotic stress method has been described in detail by Rand and co-workers in several papers (Rau et al. 1984; Parsegian et al. 1986; Rand et al. 1988, 1990; Rau and Parsegian 1992). Osmotic stress is the controlled removal of water from the system under investigation: the system is brought into contact with a polymer solution of known osmotic pressure and the structure of the phase is determined by X-ray diffraction experiments. In the present case, osmotic stress experiments were performed by equilibrating overnight the DOPE in excess of PEG (and/or dextran) solutions whose osmotic pressures (Π) have been directly measured (Parsegian et al. 1986). PEG solutions were prepared over a range of trehalose concentrations. Owing

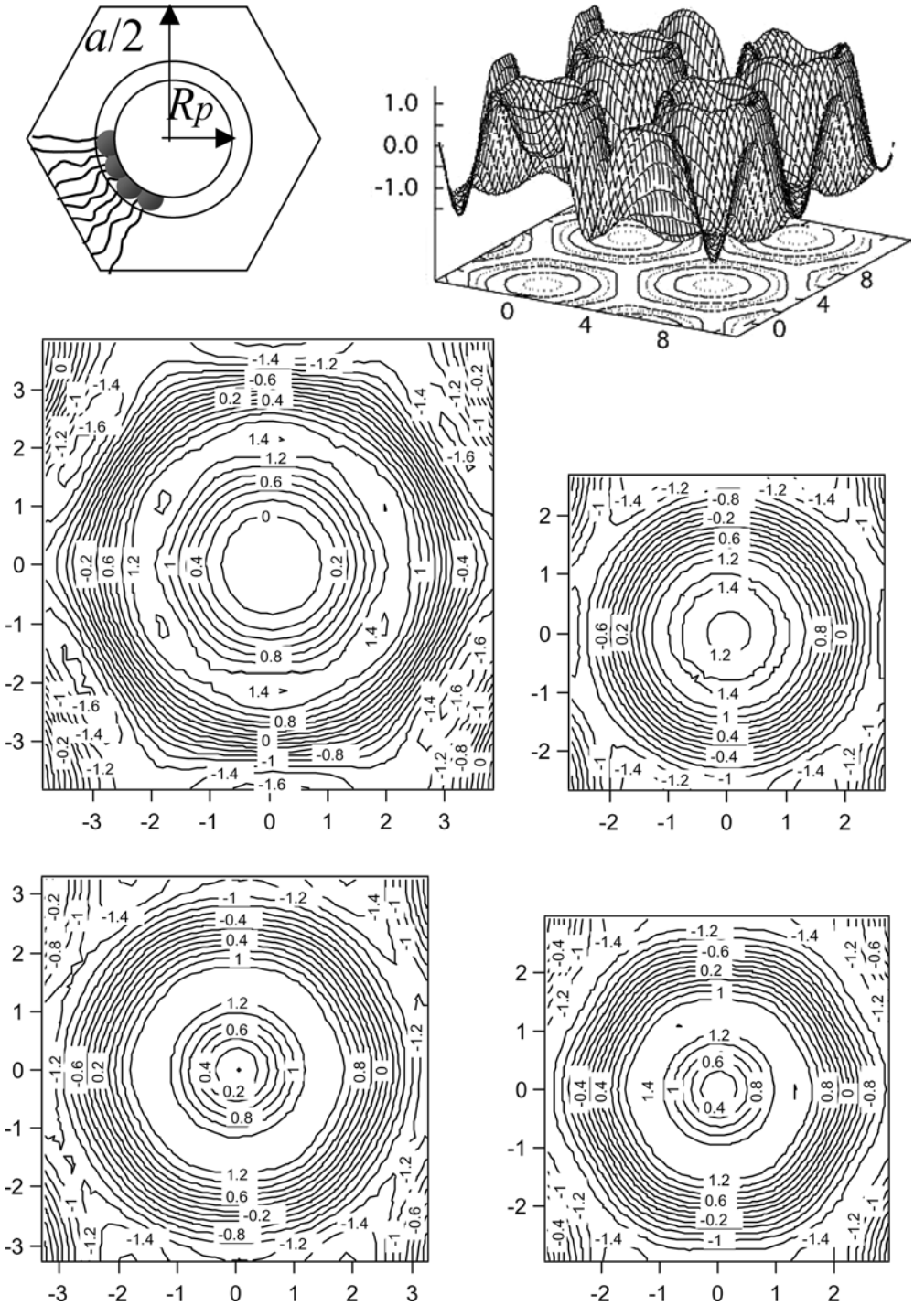

Fig. 1 Reconstructed electron density maps of the hexagonal phase for some DOPE samples equilibrated in excess PEG solutions at different osmotic stress at 25 °C. *First line*, *left side*: schematic representation of the 2D hexagonal unit cell. The *continuous lines* indicate the circular head-group contour. The dimensions *a*, which corresponds to the unit cell dimension, and R_p, the mean aqueous core radius, are indicated. *First line*, *right side*: 3D view of the electron density reconstruction of the H_{II} phase for DOPE equilibrated in pure water. *Second and third lines*, *from left in counterclockwise direction*: 2D views of the reconstructed electron density maps of the H_{II} phase for DOPE equilibrated in pure water and under an osmotic stress of 1.6×10^6 , 3.5×10^6 and 7×10^6 Pa. The density levels are all equally spaced, with an increment of 0.2. Axis dimensions are in nm

to the low trehalose solubility, the maximum PEG concentration was limited by the sugar concentration. In pure water, at 25 °C, it was possible to reach an osmotic pressure of 7×10^6 Pa, while in the case of the most concentrated trehalose solution (1.4 M), the maximum osmotic pressure exerted by PEG was 3×10^5 Pa.

Diffraction measurements were carried out using a Philips PW 1830 X-ray generator equipped with a Guinier-type focusing camera operating in vacuum with a bent quartz crystal monochromator. Diffraction patterns were recorded on a stack of three Kodak DEF-392 films or using a INEL CPS120 curved detector. The lipid phase was sealed in vacuum-tight cells with thin mica windows. In the absence of osmotic stress, diffraction data were collected from 20 to 80 °C, with temperature steps of 10 °C, while osmotic stress experiments were performed at 25 °C (a Haake F3 thermostat was used). In each experiment, from three to five sharp low-angle reflections were observed and their spacings measured. Under the different conditions the diffraction patterns were indexed according to the hexagonal lattice. In particular, the spacing ratios of the observed peaks were in the order $1:\sqrt{3}:2:\sqrt{7}...$ Once the symmetry of the lipid phase was found, the unit cell dimension, a, was calculated.

Sample composition and structural parameter determination

An important step in this work was the determination of the sample composition. At all trehalose compositions, and both in the presence or in the absence of external stresses, the structural parameters were directly measured from electron density profiles using the decomposition method recently described by Rappolt et al. (2003). After the X-ray raw data had been corrected for detector efficiency, profiles were determined by standard procedure (see, for example, Mariani et al. 1988 or Harper et al. 2001). The electron density maps were determined by Fourier transform of the calculated form factors $F_{h,k}$, where h,k are the Miller indices of each reflection. As X-ray data are not in absolute units, a scale normalization was introduced such that $\Sigma(F_{h,k})^2 = 1$. Therefore, the reconstructed maps, $\Delta\rho(x,y)$, are a normalized, dimensionless expression of the electron density distributions, $\rho(x,y)$:

$$\Delta\rho(\mathrm{x,y}) = \rho(\mathrm{x,y}) - \langle\rho\rangle \qquad (1)$$

where $<\rho>$ is the average value of the electron density distribution.

In the best cases, five reflections, the (1,0), (1,1), (2,0), (2,1) and (3,0), were observed. The phase information for each diffraction order is either positive or negative for a centrosymmetric electron density profile such as occurs for the hexagonal phase. The best phasing choice for the inverted hexagonal phase (+ − − + +) was taken from Harper et al. (2001). We also checked all the other phase combinations, but they lead to improper structural features such as a high-density hydrocarbon core or a non-uniform electron density for the aqueous compartment. Some electron density maps are shown in Fig. 1. The circular head-group contour can be easily appreciated, but other important features are the flat shape of the aqueous core, the rather constant density along the head-group contour and the scattering density minimum observed in the region far away from the cylinder surfaces. This is the region where the lipid

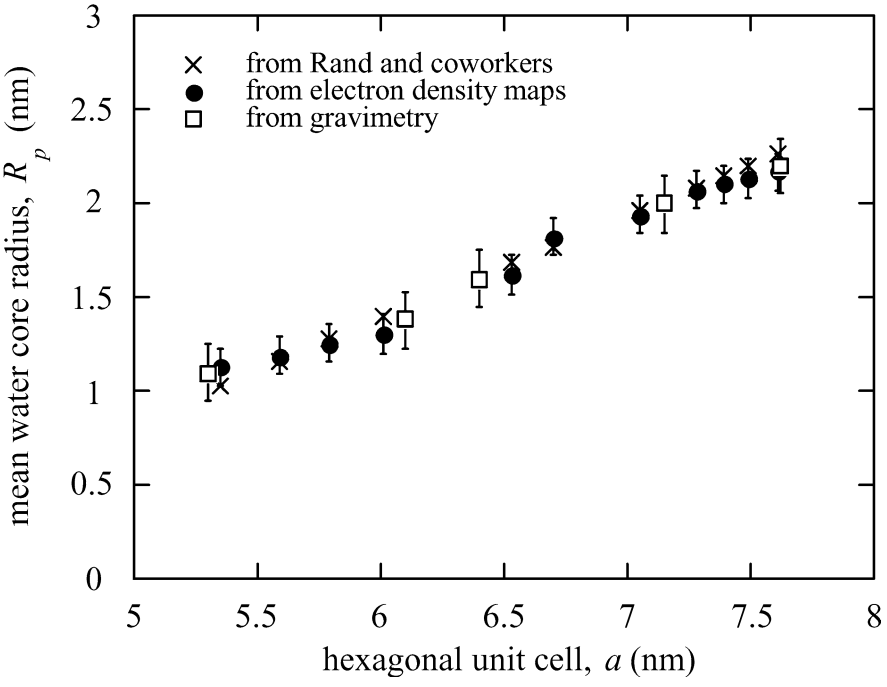

Fig. 2 Relationship between the mean aqueous core radius, R_p (measured from electron density maps), and the unit cell dimension, a, of the H_{II} phase for DOPE samples equilibrated in excess PEG solutions at different osmotic stress at 25 °C. As indicated, *crosses* correspond to radii derived by interpolating data reported by Rand and co-workers (see, for example, Leikin et al. 1996; Fuller and Rand 2001). *Squares* refer to radii calculated from gravimetrically prepared samples using the Luzzati approach (Luzzati 1968)

chains have to stretch furthest; as a plausible explanation it has suggested that low-electron-density terminal methyl groups of each DOPE chain are preferentially partitioning into those regions, particularly at high hydration levels (Turner and Gruner 1992). Owing to the introduced normalization, electron density maps are not in an absolute scale; therefore, even considering the maps obtained at the higher resolution, no information about possible effects of trehalose on the electron densities of the water compartment can be derived.

According to Rappolt et al. (2003), the electron density maps can be used to derive the mean aqueous core radius R_p, which can be directly measured as the mean distance from the center of the rod to the maximum of the electron density map (i.e., where the phosphorus groups are expected to be located). The reliability of this determination has been discussed by Rappolt et al. (2003): they found that if at least the first five peaks of the inverse hexagonal phase are used to reconstruct the electron density distribution, the position of the maximum of the electron density map (i.e., of the phosphorus groups) can be interpreted as the location of the so-called Luzzati interface, i.e. the interface which divides the hydrophobic and the hydrophilic compartments in the cell (see Luzzati 1968), within 0.1 nm. However, the maximum peak position of the electron density shifts significantly when only the first three or four reflections are taken into account in the reconstruction process. Nevertheless, Rappolt and co-workers demonstrated that very low resolution data may also be used to estimate R_p: they found that the mean water core radius is systematically underestimated in a three-peak analysis, with a stable scaling factor of 0.112 ± 0.002 nm (Rappolt et al. 2003).

In DOPE samples prepared in excess sugar solutions, the quality of the proposed approach has been assessed by comparing the mean value of the aqueous core radius derived from electron density maps to previously published data (Leikin et al. 1996; Fuller and Rand 2001) or to radii calculated using the Luzzati approach (Luzzati 1968) from X-ray data on a series of gravimetrically prepared samples. As shown in Fig. 2, errors in the estimated water core radii were lower than 5%. Thus, the position of the maximum peak position in the electron density can be interpreted as the location of the Luzzati interface. Note that according to the results obtained by Rappolt and co-workers (2003), we also included in our analysis those R_p values obtained from three-peak reconstruction (as detected in dehydrated samples), taking into account the above-mentioned scaling factor.

According to the decomposition of the sample into hydrophobic and hydrophilic compartments, the area per lipid at the lipid/water interface, S_{lip}, can then be calculated as:

$$S_{lip} = v_{lip}\left(2\pi R_p / \left(a^2\left(\sqrt{3}/2\right) - \pi R_p^2\right)\right) \quad (2)$$

where v_{lip} is the DOPE molecular volume. It should be noted that just by increasing the value of the radial distance in Eq. (2) (R_i instead of R_p), the cross-sectional area can be determined at any position along the

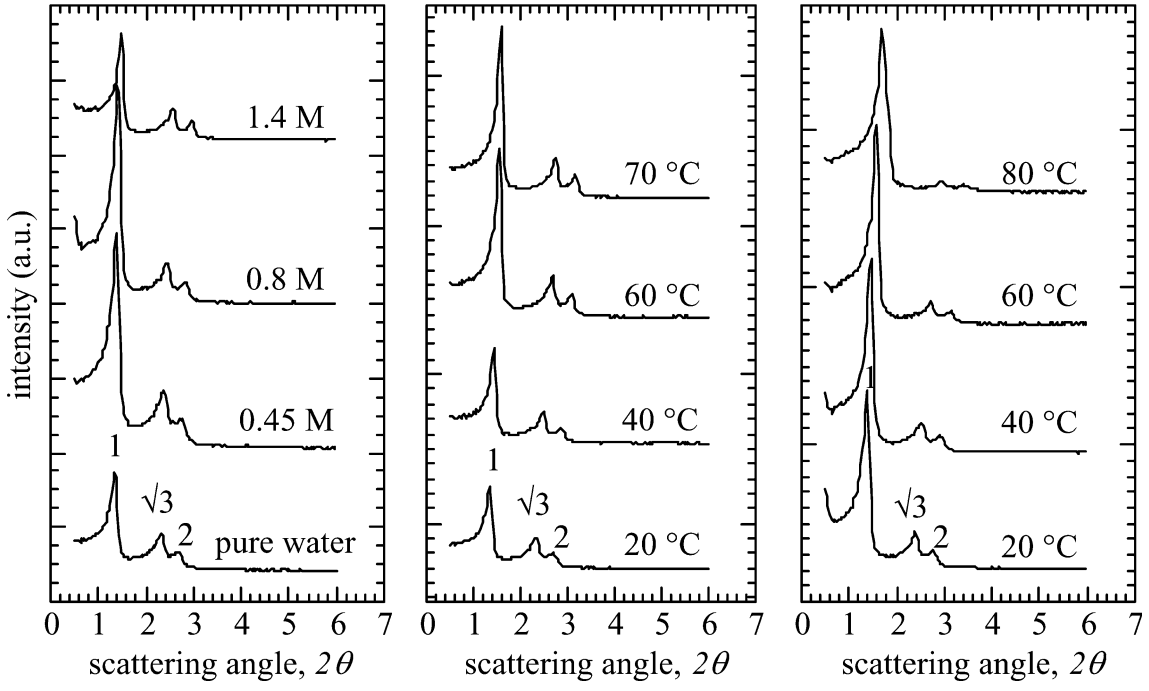

Fig. 3 Selected X-ray diffraction patterns measured from DOPE samples in excess solutions at different experimental conditions. *Left panel*: diffraction patterns obtained at different trehalose concentrations at 20 °C. *Central panel*: diffraction patterns obtained as a function of temperature for DOPE in pure water. *Right panel*: diffraction patterns obtained as a function of temperature in 0.8 M trehalose. The H_{II} peak indexing is shown

lipid chain (S_i instead of S_{lip}). The sample volume concentration of the lipidic moiety, ϕ_{lip}, can be obtained by:

$$\phi_{lip} = 2\,(a^2(\sqrt{3}/2) - \pi R_p^2)\,/\,(\sqrt{3}a^2) \quad (3)$$

Considering the presence of trehalose in the aqueous solution, and on the assumption that the trehalose composition within the aqueous compartment of the hexagonal lattice is the same as that of the reservoir (see the Discussion section for details), the water volume fraction in each sample, ϕ_w, can be determined by:

$$\phi_w = (1 - \phi_{lip})\left(1 - \frac{v_{tre}XN}{10^{27}}\right) \quad (4)$$

where $v_{tre} = 0.355$ nm^3 is the molecular volume of trehalose [as determined from trehalose solution densities (Lide 1996)], X is the trehalose concentration of the bathing solution (in mol L^{-1}) and N is Avogadro's number. Then, the number of water molecules per lipid, n_w, and the volume of water per lipid, V_w, can be calculated by:

$$n_w = \frac{v_{lip}\phi_w}{v_w\phi_{lip}}, \quad V_w = n_w v_w \quad (5)$$

where v_w is the water molecular volume.

Results

The effects of trehalose on DOPE structural properties were analyzed under two different conditions: (1) DOPE in excess of trehalose at different temperatures, and (2) under osmotic stress, i.e. considering DOPE in excess PEG solutions at different trehalose concentrations.

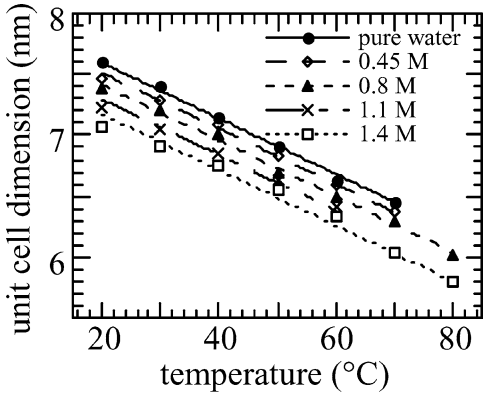

Fig. 4 Temperature dependence of H_{II} unit cell of fully hydrated DOPE samples in different trehalose solutions. Data have been fitted with a linear regression. From the slope, the thermal expansion coefficient, $\alpha_a = \mathrm{d}\,a/\mathrm{d}\,T$, has been obtained for the different solutions: −0.024 nm/°C (pure water); −0.022 nm/°C (0.45 M trehalose); −0.023 nm/°C (0.8 M trehalose); −0.022 nm/°C (1.1 M trehalose); −0.023 nm/°C (1.4 M trehalose). In the figure the average value of $\alpha_a = -0.023$ nm/°C has been used to fit each data set

DOPE in excess of trehalose solutions

Some examples of X-ray diffraction patterns obtained in excess of trehalose solutions at different temperatures are shown in Fig. 3. At first glance, two results are evident: first, no phase transitions occur; and second, the changes in the peak position indicate that the hexagonal lattice parameter reduces when the temperature or sugar concentration increase. In Fig. 4 the unit cell dimensions, measured at different trehalose concentrations, are shown as a function of temperature. It is noteworthy that a unique thermal expansion coefficient, $\alpha_a = -0.023$ nm/°C, can be used to fit the complete dataset, suggesting that the thermal effect is unaltered by the presence of trehalose.

As described in the Materials and methods section, the sample composition at 20 °C has been obtained by directly measuring the mean aqueous core radius, R_p, from reconstructed electron density maps (see Figs. 1 and 2) and calculating the aqueous volume fraction by Eqs. (2) and (4). The volume fraction of the aqueous compartment in the hexagonal phase is given in Fig. 5 as a function of the trehalose concentration in the bulk solution. In particular, the volume concentration of the aqueous moiety drops from 0.32 in pure water (which corresponds to the hexagonal lattice parameter of 7.61 nm) down to 0.28 in 1.4 M trehalose (measured hexagonal unit cell of 7.06 nm), clearly indicating that the sugar induces DOPE dehydration.

Using Eqs. (2) and (5), some important molecular parameters at 20 °C have been determined as a function of sugar concentration and are shown in Fig. 6. It can be seen that the surface-per-polar head at the lipid/water interface, S_{lip}, progressively decreases as the sugar concentration is increased. This indicates that trehalose leads to a continuous shrinking of the polar rods. Considering that also the cross-sectional area at the methyl terminal end of the hydrocarbon chains, S_t, depends on trehalose concentration, a continuous change of the DOPE molecular shape can be inferred. Moreover, the decrease of the number of water molecules per DOPE (calculated under the hypothesis of

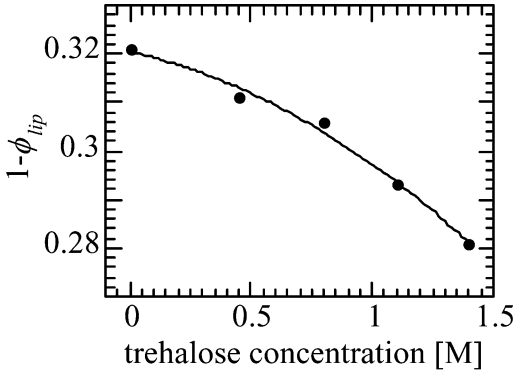

Fig. 5 Trehalose concentration dependence of the volume fraction of the aqueous compartment ($1-\phi_{lip}$) in the DOPE H_{II} phase in excess solution. The *line* is a guide to the eyes

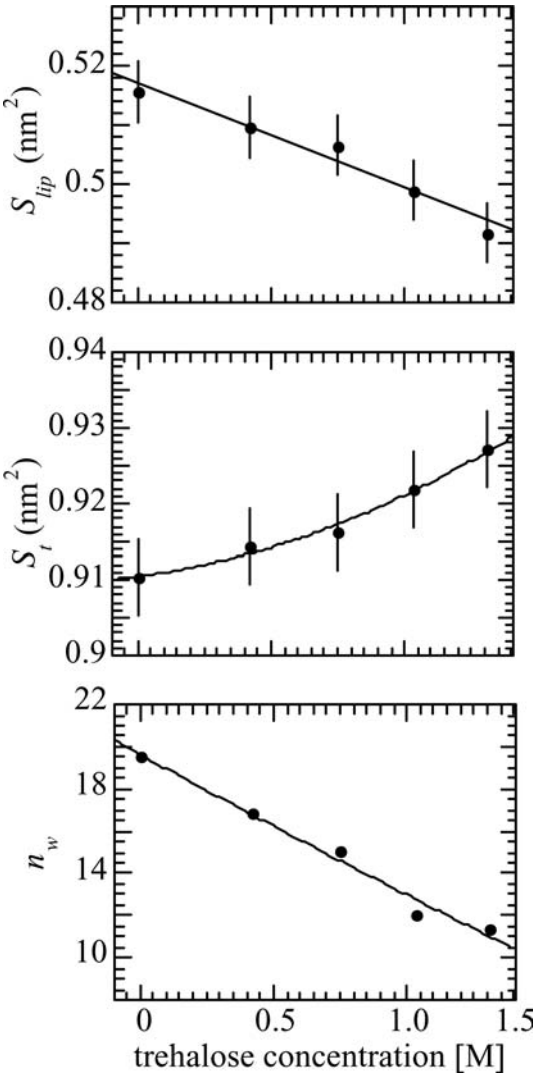

Fig. 6 Trehalose concentration dependence of some structural parameters of the DOPE H_{II} phase in excess solution. *Upper panel*: molecular cross-sectional area at the lipid/water interface, S_{lip}. *Middle panel*: molecular cross-sectional area at the terminal methyl group, S_t. *Lower panel*: number of water molecules per DOPE molecule, n_w. *Lines* are guides to show the general trend

homogeneous distribution of trehalose; see Eq. 5) as a function of the sugar concentration directly confirms the dehydration effect, as previously observed for other lipids (Crowe et al. 1984; Crowe et al. 1987; Crowe and Crowe 1988; Koynova et al. 1989; Sanderson et al. 1991; Koynova and Caffrey 1994; Tsonev et al. 1994; Cordone et al. 1998; Mariani et al. 1999).

Further, also the characteristics of the pivotal surface have been taken into account. Such a surface is defined to be the location on the molecule whose area remains invariant upon isothermal bending. This means that either side of the pivotal surface remain fixed as the interface is bent (Templer et al. 1998).

Templer and co-workers (1998) derived two equations which relate the pivotal surface to the lattice parameter of the hexagonal phase:

$$a = \frac{2}{\phi_{\mathrm{lip}}\left(S_{\mathrm{n}}/v_{\mathrm{lip}}\right)}\sqrt{\frac{2\pi}{\sqrt{3}}\left(1-\frac{v_{\mathrm{n}}}{v_{\mathrm{lip}}}\phi_{\mathrm{lip}}\right)} \tag{6}$$

and:

$$R_{\mathrm{n}} = \sqrt{\left(\frac{v_{\mathrm{n}}}{S_{\mathrm{n}}}\right)^2 + \frac{\sqrt{3}a^2}{2\pi}} - \frac{v_{\mathrm{n}}}{S_{\mathrm{n}}} \tag{7}$$

where S_n is the molecular area at the pivotal plane, v_n is the molecular volume between the pivotal plane and the end of the lipid chain, and R_n is the radial distance from the pivotal surface to the center of the aqueous channel. Therefore we derived the characteristics of the pivotal surface by fitting a versus $1-\phi_{lip}$ (which in turn depends on trehalose concentration) using Eq. (6). The results are shown in Fig. 7 (upper panel). The goodness of the fit indicates that the DOPE dehydration induced by trehalose in excess water conditions leads to a continuous deformation of the hexagonal phase, which consists of a rearrangement of the molecular packing geometry around the pivotal position along the phospholipid

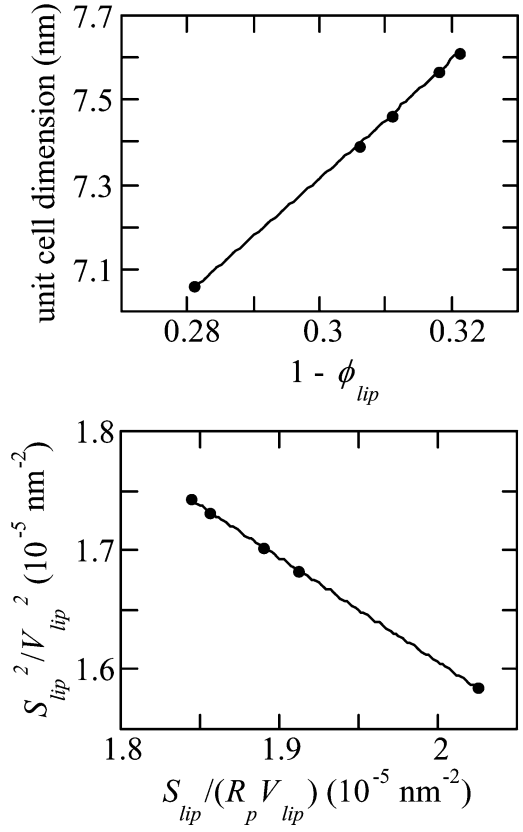

Fig. 7 Determination of the pivotal surface characteristics of the H_{II} phase of DOPE in excess trehalose solutions. *Upper panel*: Templer fit of the unit cell plotted versus the estimated volume concentration of the aqueous compartment, $(1-\phi_{lip})$ (see Eq. 6). The best fit parameters are $S_n = 0.719 \pm 0.040$ nm^2 and $v_n = 0.680 \pm 0.040$ nm^3. *Lower panel*: Rand diagnostic fit of the S_{lip}^2 versus S_{lip}/R_p (see Eq. 8). Note that data have been normalized for the lipid molecular volume (Fuller and Rand 2001). The best fit parameters are $S_{pp} = S_n = 0.715 \pm 0.046$ nm^2 and $v_{pp} = v_{lip} - v_n = 0.540 \pm 0.070$ nm^3

molecule. At the pivotal surface, S_n is 0.719 ± 0.040 nm^2 and v_n is 0.680 ± 0.040 nm^3. The corresponding averaged R_n is in turn about 3 nm. Note that for DOPE in excess of water, Rand and co-workers (Fuller and Rand 2001; Szule and Rand 2003) also found a radial distance from the pivotal surface to the center of the water channel of about 3 nm.

According to Rand and co-workers, the proof that the area remains constant at some fixed position during the bending can be obtained by considering that the molecular area, S, and the radius of curvature, R, at any cylindrical surface, separated by a volume v per lipid molecule from the Luzzati plane, are related by (Rand and Fuller 1994, Leikin et al. 1996; Chen and Rand 1998; Fuller and Rand 2001; Szule and Rand 2003):

$$S^2 = S_{lip}^2 + 2v\left(S_{lip}/R_p\right) \quad (8)$$

Therefore, if the plot of ${S_{lip}}^2$ versus S_{lip}/R_p is a straight line, the system has a dividing surface of constant area, the pivotal plane, and the slope and the intercept of the plot give both the position of the pivotal plane, R_p, or the volume, v_{pp} (note that $v_{pp} = v_{lip} - v_n$), respectively, and the cross-sectional molecular area at that plane, $S_{pp} = S_n$. The plot obtained in the present case is shown in the lower panel of Fig. 7; the observed behavior confirms the presence and the location of the pivotal plane. As a final note, we think it interesting to observe that the obtained values are in agreement with data reported by Rand and co-workers for DOPE in pure water (Kozlov et al. 1994; Leikin et al. 1996; Chen and Rand 1998; Fuller and Rand 2001; Szule and Rand 2003).

Osmotic stress on the DOPE at different trehalose concentrations

The effects of trehalose on DOPE structural properties were further analyzed by osmotic stress experiments. Controlling the water activity makes it possible to evaluate the sugar effects on the lipid phase during dehydration phenomena. Some X-ray diffraction profiles obtained at different osmotic pressures exerted by PEG are shown in Fig. 8. It can be observed that the hexagonal phase still exists even at the higher applied pressures. The hexagonal unit cell dependence on the osmotic pressure exerted by PEG at different sugar concentrations is shown in Fig. 9a, and confirms that the presence of trehalose induces a shrinking of the hexagonal lattice.

The composition of each sample was then determined by measuring from the reconstructed electron density maps the mean aqueous core radius, R_p, and by applying Eqs. (3) and (4). The different structural parameters have been then calculated using Eqs. (2) and (5). The results are shown in Fig. 9b–d. It is evident that the sugar strongly affects the curvature of the monolayer ($1/R_p$), reducing the area-per-molecule at the lipid/water interface and the number of water molecules per DOPE inside the aqueous channel.

Applying Eqs. (6), (7) and (8) to data obtained at constant trehalose concentration as a function of the osmotic stress exerted by PEG, the characteristics of the pivotal surface in the different experimental conditions were also determined. The results are shown in Fig. 10. The goodness of the fits, both using equations from Templer et al. (1998) (upper panel) and Rand

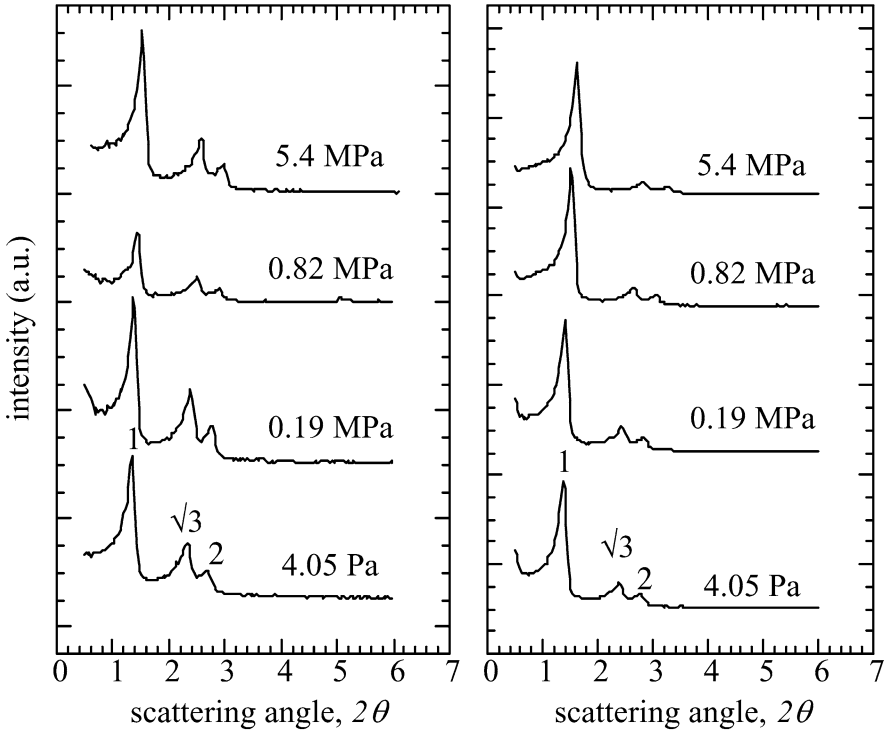

Fig. 8 Selected X-ray diffraction profiles obtained at different osmotic pressures exerted by PEG on DOPE samples equilibrated in excess of pure water (*left panel*) and in excess of 0.8 M trehalose solution (*right panel*). The corresponding osmotic pressures are indicated. H_{II} peak indexing is also shown

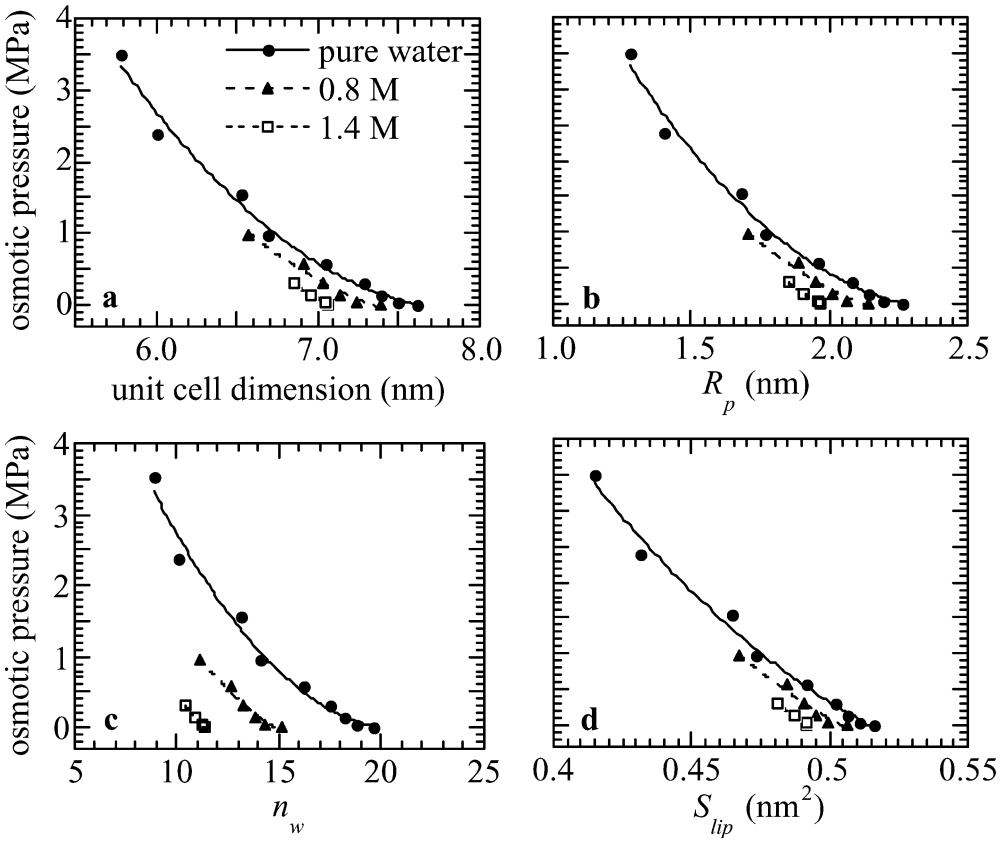

Fig. 9 Dependence on osmotic pressure of structural parameters of the H_{II} phase of DOPE in pure water and in 0.8 and 1.4 M trehalose solutions: (**a**) unit cell dimensions; (**b**) radius of the mean aqueous core, R_p; (**c**) number of water molecules per DOPE molecule, n_w; (**d**) molecular cross-sectional area at the lipid/water interface, S_{lip}. *Lines* are guides to the eyes to show the general trend

and co-workers (Rand and Fuller 1994; Leikin et al. 1996; Chen and Rand 1998; Fuller and Rand 2001; Szule and Rand 2003) (lower panel), indicates the presence of the pivotal surface within the DOPE molecules at all the investigated trehalose concentrations. In Fig. 11 the cross-sectional area at the pivotal position, S_n, and the radial distance from this surface to the center of the aqueous channel, R_n, are shown as a function of sugar concentration. As suggested by results obtained in excess trehalose solutions (see Fig. 6), it is confirmed that the sugar affects only slightly the cross-sectional area at the pivotal plane. The same figure also shows the radial distance from the pivotal surface to the center of the aqueous channel, R_n, as a function of the trehalose concentration. As expected, the location of the pivotal surface depends on the osmotic stress induced by PEG.

It should be noted that the n_w parameter shown in Fig. 9 (as well as in Fig. 6) has been calculated assuming that the trehalose composition within the aqueous compartment of the hexagonal lattice is the same as that of the reservoir. If trehalose partitions unequally between these aqueous compartments, then the composition of the aqueous channels is unknown and the number of water molecule per DOPE cannot be determined. Note that the primary data, the change in lattice dimension with trehalose composition, seem to suggest that trehalose is partitioning unequally between reservoir and lattice and is acting osmotically.

However, dual-solvent stress experiments prove that the trehalose effect is not purely osmotic. Two results should be emphasized. First, in excess of water at 20 °C, DOPE enters a lamellar phase when the osmotic pressure of the bathing solution is higher than 3×10^6 Pa (Gawrish et al. 1992). We observed that this transition can be induced using PEG 8,000 or 20,000 or using a mixture of PEG and dextran. By contrast, no phase transitions have been detected when the osmotic stress experiment is performed in 0.1 M trehalose (note that the presence of trehalose limits the attainable osmotic pressure to 5.0×10^6 Pa). This result agrees with the observation that no phase transitions occur in the monoolein/water system when dehydration is performed in the presence of trehalose (Mariani et al. 1999; Saturni et al. 2001), and with the similar protective effect exerted by sucrose on DOPE at moderate and low hydration (Shalaev and Steponkus 2001). Second, the DOPE dehydration process has been followed in the presence of trehalose and of different combinations of PEG and dextran. The nominal osmotic stress exerted on DOPE was calculated as the sum of the partial osmotic pressures exerted by the different components (Perry et al. 1980; Rau et al. 1984; Parsegian et al. 1986; Rand et al. 1988; Rand et al. 1990; Rau and Parsegian 1992; see also http://aqueous.labs.brocku.ca/osfile.html). Note that, in this calculation, trehalose was considered to fully dissolve in the bulk compartment. In Fig. 12 the measured DOPE hexagonal unit cell is shown as a function of the

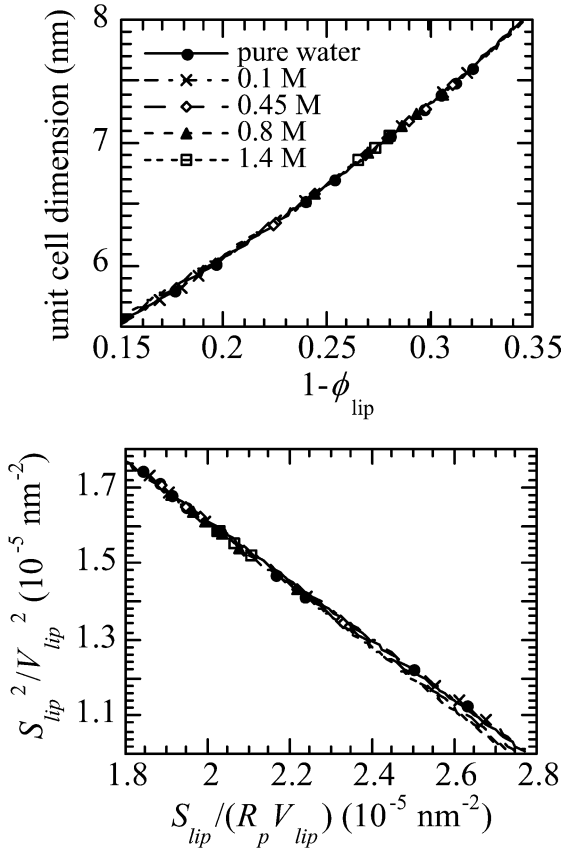

Fig. 10 Determination of the pivotal surface characteristics of the H_{II} phase of DOPE under osmotic stress at different trehalose concentrations. *Upper panel*: Templer fit of the unit cell plotted versus the volume concentration of the aqueous compartment, $(1-\phi_{lip})$ (see Eq. 6). The best-fit parameters are: pure water, $S_n = 0.698 \pm 0.003$ nm^2 and $v_n = 0.746 \pm 0.006$ nm^3; 0.1 M trehalose, $S_n = 0.696 \pm 0.003$ nm^2 and $v_n = 0.754 \pm 0.005$ nm^3; 0.45 M trehalose, $S_n = 0.704 \pm 0.005$ nm^2 and $v_n = 0.732 \pm 0.009$ nm^3; 0.8 M trehalose, $S_n = 0.707 \pm 0.006$ nm^2 and $v_n = 0.721 \pm 0.016$ nm^3; 1.4 M trehalose, $S_n = 0.715 \pm 0.005$ nm^2 and $v_n = 0.700 \pm 0.060$ nm^3. *Lower panel*: Rand diagnostic fit of S_{lip}^2 versus S_{lip}/R_p (see Eq. 8). Note that data have been normalized for the lipid molecular volume (Fuller and Rand 2001). The best-fit parameters are: pure water, $S_{pp} = S_n = 0.697 \pm 0.002$ nm^2 and $v_{pp} = v_{lip} - v_n = 0.485 \pm 0.005$ nm^3; 0.1 M trehalose, $S_{pp} = 0.695 \pm 0.002$ nm^2 and $v_{pp} = 0.479 \pm 0.007$ nm^3; 0.45 M trehalose, $S_{pp} = 0.701 \pm 0.004$ nm^2 and $v_{pp} = 0.497 \pm 0.005$ nm^3; 0.8 M trehalose, $S_{pp} = 0.703 \pm 0.004$ nm^2 and $v_{pp} = 0.505 \pm 0.007$ nm^3; 1.4 M trehalose, $S_{pp} = 0.704 \pm 0.006$ nm^2 and $v_{pp} = 0.506 \pm 0.004$ nm^3

nominal osmotic pressure of the solution. It is evident that PEG and PEG/dextran solutions have the same effect on the lattice parameter, while trehalose-containing solutions (pure trehalose and PEG/0.8 M trehalose) affect the unit cell dimension in a different manner, suggesting that trehalose should have a further effect than merely osmotic.

It is obvious that the changes in trehalose solubility with PEG concentration shows that its activity and therefore its distribution between reservoir and lattice is at least complicated. An unequal partitioning might be expected, in particular in extremely stressed conditions (high PEG and sugar concentrations), when the trehalose dimension approaches the dimension of the aqueous channel.

Discussion

The aim of this study is to improve the comprehension of the molecular mechanisms which govern the stabilization of lipid structures induced by sugars when the water removal phenomenon occurs. In particular, trehalose is well known for its stabilizing effect and protective role against dryness of biological systems (Crowe et al. 1987; Crowe and Crowe 1988; Koynova et al. 1989; Sanderson et al. 1991; Koynova and Caffrey 1994; Tsonev et al. 1994; Cordone et al. 1998; Mariani et al. 1999). Different mechanisms have been suggested to explain its action, such as the osmotic dehydration of the lipid phases due to sugar exclusion from the fraction of water inside the rods (Koynova et al. 1997), or the replacement of water by sugar molecules which make hydrogen bonds with the hydrophilic surfaces (Crowe et al. 1987; Crowe and Crowe 1988; Crowe 2002). Moreover, trehalose has been suggested to act as a kosmotropic reagent, stabilizing the structure of water and modifying its behavior at the lipidic interface according to the Hofmeister effect (Sanderson et al. 1991). Very recently, it has been also proposed that the highly viscous sugar solutions create a rigid immobile matrix around and inside the lipid phase, such that phase transitions (which require rearrangements of the lipid molecules) are greatly impeded (Shalaev and Steponkus 2001).

In the present case, the structural properties of the DOPE hexagonal phase have been analyzed in the presence of trehalose. Two different cases have been considered, i.e. DOPE in excess of water and in the presence of increasing trehalose concentrations (see Fig. 3), and DOPE in trehalose solutions and in the presence of increasing PEG concentrations (see Fig. 8). In the first condition, a net reduction of the unit cell as a function of trehalose concentration is observed, indicating that the presence of sugar leads to a shrinking of the polar rods (see Fig. 4). The effect is visible at all the investigated temperatures (from 20 to 80 °C). Noteworthy is the fact that the (negative) thermal expansion coefficient is independent of sugar concentration, suggesting that the temperature effect on the hexagonal phase should be mainly related to the thermal behavior of the lipidic component. Many PCs, such as L-α-dipalmitoyl-phosphatidyl-choline (DOPC), L-α-dimyristoyl-phosphatidyl-choline (DMPC) and L-α-distearoyl-phosphatidyl-choline (DSPC), have been extensively studied by calorimetry (Cevc 1991; Tenchov et al. 2001; Heerklotz and Seelig 2002). In particular, the linear expansion coefficient α_l [$\alpha_l = 1/l(\Delta l/\Delta T)$, where l represents the membrane thickness], calculated either from ^{2}H NMR or from X-ray or neutron scattering data (Seelig and Seelig 1974; Salmon et al. 1987; Sankaram and

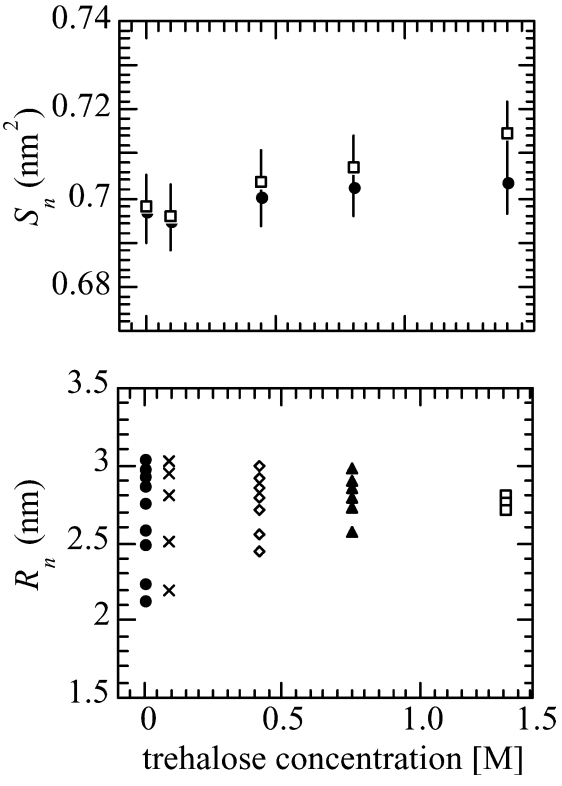

Fig. 11 Dependence of the pivotal surface characteristics on trehalose concentration. *Upper panel*: molecular cross-sectional area at the pivotal plane, S_n, obtained using the method of analysis reported by Fuller and Rand (2001) (*full circles*) and by Templer and co-workers (1998) (*open squares*). *Lower panel*: distance from the pivotal surface to the center of the aqueous channel, R_n. Note that at constant trehalose molarity this distance changes with osmotic pressure (under osmotic stress, R_n decreases)

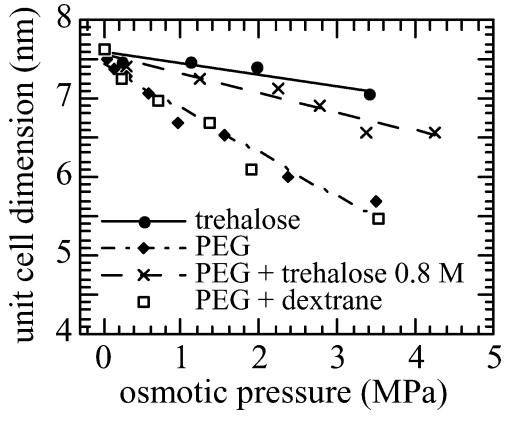

Fig. 12 Dependence of the H_{II} unit cell of DOPE on the nominal osmotic pressure exerted by trehalose, PEG, PEG and 0.8 M trehalose, and PEG and dextran solutions. *Lines* are guide to the eyes to show the general trends

Thompson 1992), ranges from -1.5×10^{-3} °C^{-1} for DMPC to -2.9×10^{-3} °C^{-1} for DSPC. In the present case, a linear expansion coefficient of -3×10^{-3} °C^{-1} has been derived. The good agreement with values obtained for PCs confirms that the thermal effect is related to the shrinking of the hydrocarbon chain length upon thermal excitation (Heerklotz and Seelig 2002).

The structural parameters of the hexagonal phase forming in the presence of trehalose were obtained both in excess of water and under osmotic stress. In particular, the lipid sample composition in the different experimental conditions was directly derived from the average water core radius (R_p) measured from the reconstructed electron density maps (see Figs. 1, 5 and 9). As a result, it is observed that increasing the sugar concentration increases the curvature of the monolayer, while the DOPE cross-sectional area reduces at the lipid/water interface, and sensibly increases at the hydrocarbon chain ends (see Figs. 6 and 9). Moreover, assuming that trehalose partitions equally between the aqueous compartment of the hexagonal lattice and that of the bathing solution, the number of water molecule per DOPE inside the water channel can be calculated. This number decreases as a function of sugar content.

Dual-solvent stress experiments, which confirm the absence of phase transitions in the presence of the sugar, definitely indicate that trehalose should have a further effect than merely osmotic (see Fig. 12 and Shalaev and Steponkus 2001). The observed structural consequences cannot be due only to an unequal partition of trehalose

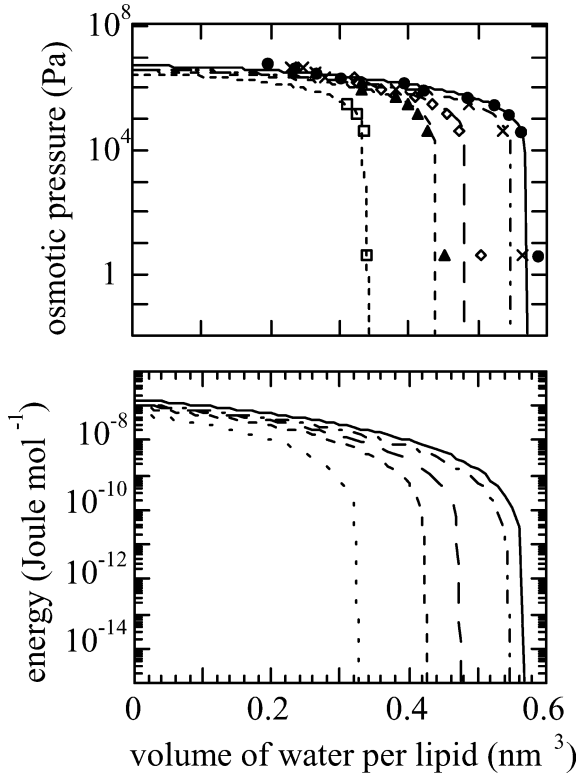

Fig. 13 *Upper panel*: osmotic pressure dependence on the volume of water per DOPE molecule, V_w, measured at different trehalose concentrations in the H_{II} phase. *Lower panel*: change of the overall free energy of the hexagonal phase (as determined in different trehalose solutions) as a function of V_w. *Symbols* as in Fig. 10. *Lines* are visual guides to show the general trend

between the bulk of the solution and the solvation layers of the lipid surfaces. However, since independent experimental data on trehalose partitioning are hard to obtain, we are forced to make some simple assumptions. For sake of clearness we will assume in the following that the trehalose composition within the aqueous compartment of the hexagonal lattice is the same as that of the bulk solution. Note, however, that owing to the expected complicated behavior in extremely dehydrated conditions, the data at higher investigated stresses will not be used in the energetic analysis of the hexagonal phase.

With the above accord, osmotic data have been analyzed following the method described by Rand et al. (1990). The osmotic pressure has been first plotted versus the volume of water per DOPE (calculated from Eqs. 4 and 5), as shown in Fig. 13 (upper panel). Then, by numerical integration of the osmotic pressure (Π) in dependence on the volume of water per lipid molecule, the overall free energy ($\Delta g = g - g_0$) of the system under dehydration has been obtained:

$$g = g_0 - \int \Pi \, \mathrm{d}V_\mathrm{w} \tag{9}$$

Free energy data at different trehalose concentrations are shown in the lower panel of Fig. 13. This energy represents the work required to dehydrate the hydrophilic surfaces of the DOPE monolayer, and includes, among others, the cost of bending the lipid layer (bending energy) and the cost of lateral packing of the lipid molecules (stretching energy) (Templer et al. 1995; Vacklin et al. 2000).

If the free energy is referred to the pivotal surface, which has a molecular cross-sectional area invariant upon isothermal bending, one can exclude as a first approximation any energy due to lateral monolayer stretching. The quadratic form of the bending energy per unit area [i.e., the energy of bending the pivotal surface from the spontaneous radius of curvature R_0 to a different radius R_n against the rigidity bending modulus k_c (Helfrich 1973)] is:

$$\Delta g = \frac{1}{2} k_\mathrm{c} \left(\frac{1}{R_\mathrm{n}} - \frac{1}{R_0} \right)^2 \tag{10}$$

and can be used to describe the work of water removal from the hexagonal lattice. In Eq. (10), the bending modulus includes a factor 2 (see below), which is appropriate to describe the energy for bending two monolayers; this conversion allows the comparison with the bending energy of a bilayer under the assumption that the two leaflets are uncoupled during bending.

As demonstrated by Rand et al. (1990), the contribution of the bending energy to the osmotic pressure of the lattice is:

$$\Pi = K_0 \left(\frac{1}{R_\mathrm{n}} - \frac{1}{R_0} \right) \left(-\frac{1}{R_\mathrm{n}^2} \right) \left(\frac{2}{S_\mathrm{n}} \right) \tag{11}$$

where K_0 is the monolayer bending modulus per molecule ($k_\mathrm{c} = 2K_0/S_\mathrm{n}$), from which a linear relationship between ΠR_n^2 versus $1/R_\mathrm{n}$ can be obtained (Rand et al. 1990; Gawrish et al. 1992):

$$\Pi R_\mathrm{n}^2 = k_\mathrm{c} \left(\frac{1}{R_0} - \frac{1}{R_\mathrm{n}} \right) \tag{12}$$

Osmotic stress data versus $1/R_\mathrm{n}$, for pure water and trehalose solutions, are given in Fig. 14. The data show remarkable linearity for all the osmotic pressures. The same behavior has been observed at all the sugar concentrations analyzed. By linear fitting data through Eq. (12), the rigidity constant k_c and the DOPE spontaneous radius of curvature R_0 (measured at the pivotal surface) have been determined at each sugar concentration. The fitted parameters are shown in Fig. 15 as a function of trehalose concentration: an increase of the bilayer rigidity and a sensible reduction of the spontaneous radius of curvature due to the presence of trehalose is derived.

These results are remarkable: an increased spontaneous curvature of the lipid layer indicates a less efficient torque associated with head-group repulsion in balancing the torque of chain repulsion. We assume that this effect is related to a direct interaction between trehalose and DOPE [as also supported by infrared spectroscopy results (Crowe et al. 1984)], and thus, that trehalose alters directly the interface geometry. Moreover, the increased bending rigidity increases the DOPE repulsion as dehydration occurs, which is most probable due to the reduced cross-sectional area of the lipid molecules. Nevertheless, the dependence of the bending rigidity on trehalose concentration could also be related to the property of the aqueous compartment: the increased rigidity and stiffness of the sugar matrix around and inside the lipid phase, which according to the viscosity hypothesis impede the occurrence of lipid phase transitions (Shalaev and Steponkus 2001), can also account for the changes in the monolayer mechanical property.

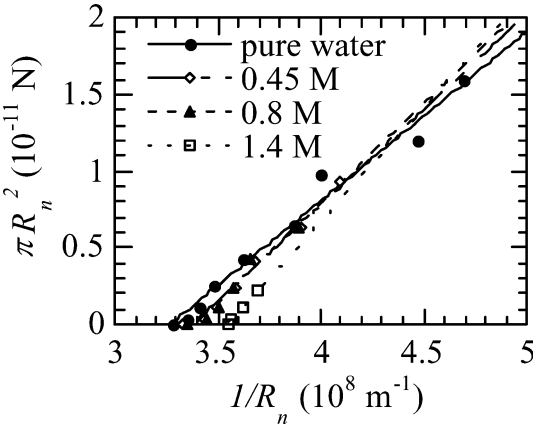

Fig. 14 Fit of the osmotic stress data (ΠR_n^2 versus $1/R_\mathrm{n}$) by Eq. (11). Fit parameters are shown in Fig. 15

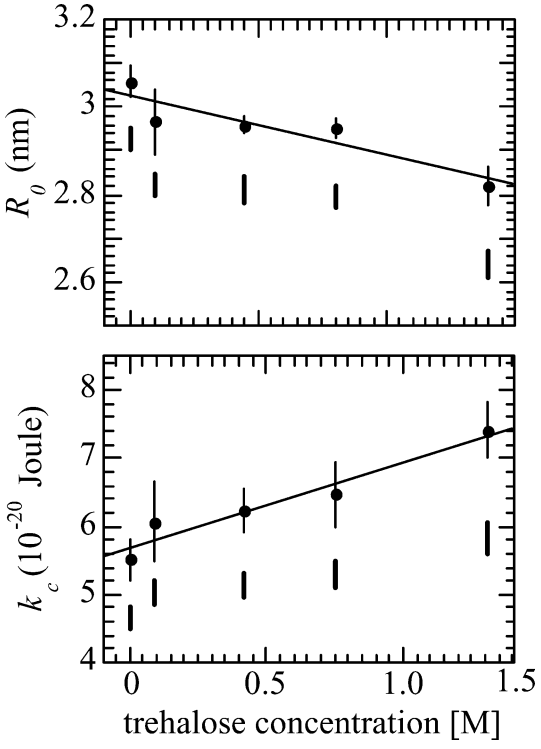

Fig. 15 Dependence on trehalose concentration of the spontaneous radius of curvature, R_0, and of the rigidity constant, k_c, of the DOPE monolayer measured at the pivotal plane (see text and Fig. 14). *Lines* are guides to show the general trend. *Solid bars* represent the spontaneous radius of curvature, R_{0n}, and the rigidity constant, k_{cn}, estimated for the neutral surface according to Leikin et al. (1996)

Whatever the origin, the changes in the monolayer mechanical characteristics reflect an increase of the free energy associated with the flattening of the DOPE hexagonal-phase monolayer into a planar bilayer conformation. In Fig. 16 the cost to unbend the lipid monolayer (Gawrish et al. 1992) is shown as a function of trehalose concentration. Obviously, the altered DOPE packing geometry is a sufficient condition for thermodynamic preference of the hexagonal over the lamellar phase, that in fact does not form under dehydration.

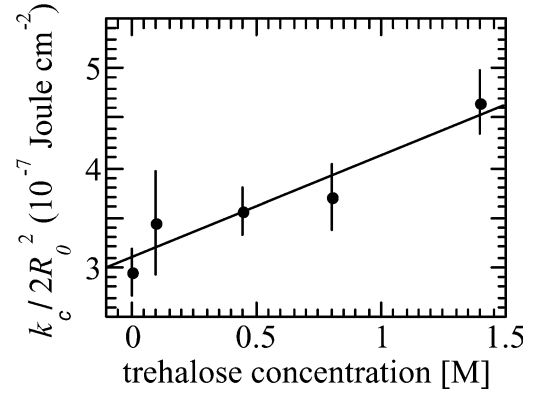

Fig. 16 Dependence on trehalose concentration of the energetic cost to unbend the lipid monolayer to the flat, $k_c/(2R_0^2)$. The *line* is a guide to show the general trend

In this work, we derived a variety of structural parameters for the DOPE hexagonal phase and we have discussed how they are affected by trehalose. Remarkably, trehalose induces highly curved DOPE which it is not possible to obtain by osmotic dehydration that would induce the hexagonal-to-lamellar phase transition (Gawrisch et al. 1992). This confirms that the trehalose effect is not purely osmotic. In this highly stressed regime, we have determined the spontaneous radius of curvature and the rigidity constant for the pivotal surface as a function of the trehalose concentration (see Fig. 15). The results indicate a simple and reasonable explanation for the additional stabilization exerted by trehalose (see Fig. 16): the altered monolayer mechanical characteristics induced by trehalose both changing the rigidity of the aqueous compartment in the lipid phase and/or directly interacting with DOPE and modifying the interface geometry, are a sufficient reason for the observed thermodynamic preference of the hexagonal over the lamellar phase, even under dehydration.

Additional note on the derivation of the mechanical monolayer characteristics

According to the large sensitivity to the form of the experimental data, in this paper much attention has been devoted to the determination of the pivotal surface position. Both Rand's diagnostic plot (Rand and Fuller 1994; Leikin et al. 1996; Chen and Rand 1998; Fuller and Rand 2001; Szule and Rand 2003) and Templer's equation (Templer et al. 1998) have been used to prove that each DOPE sample has a well-defined pivotal plane, and that the relative position is practically independent of the trehalose concentration of the bathing solution. However, even if a clear trend can be derived (see Fig. 15), the parameters which describe the energetic of the phase both in the absence and in the presence of trehalose are well inside data previously reported for DOPE (Leikin et al. 1996; Chen and Rand 1998; Fuller and Rand 2001; Szule and Rand 2003), which in fact cover a surprising large range. As clearly stated by Leikin and co-workers (1996), the determination of the spontaneous radius of curvature and of the rigidity constant of a monolayer is in fact seriously limited by the dependence of the pivotal plane position on the relationship between area compressibility and bending of the monolayer, i.e. on the deformation or the experimental technique. By contrast, unique and intrinsic properties of the lipid monolayer are the spontaneous radius of curvature and the rigidity modulus determined at the neutral plane. The neutral plane is defined as that surface where the bending and stretching (compression) deformations are energetically uncoupled, so that its position does not depend on the deformation or on the experimental techniques (Kozlov and Winterhalter 1991; Leikin at al. 1996).

As the determination of the position of the neutral plane in the H_{II} phase is a rather difficult problem, Leikin and co-workers (1996) derived two equations to estimate the elastic parameters at this surface for small deformations:

$$R_0 \approx (1+\gamma)R_{0n}; \quad k_c \approx (1+4\gamma)k_{cn} \tag{13}$$

where R_{0n} and k_{cn} are the spontaneous radius of curvature and the rigidity constant at the neutral plane, respectively, and γ is defined by k_{cn}/KR^2_{0n}. K is the lateral compressibility modulus of the monolayer and should be measured independently. In our approximate calculation, we used K values ranging from 0.10 to 0.15 N m^{-1}, as reported by Evans and Needham (1987) and as already used by Leikin and co-workers (1996) for the DOPE system. While γ is observed to change from 0.03–0.05 to 0.07–0.08 in the presence of 1.4 M trehalose, the calculated elastic parameters are shown in Fig. 15, as solid bars. It should be noted that the difference between the spontaneous radius of curvature at the pivotal and at the neutral surface is around 5%. This difference is rather small in comparison with the variation of curvature observed as a function of the trehalose concentration. Therefore, it can be concluded that the decrease of the spontaneous radius of curvature induced by trehalose is valid both for the pivotal and neutral surface. On the other hand, the difference between the rigidity constant at the pivotal and neutral planes is around 20–25% (depending on trehalose concentration). The difference is comparable with the observed bending modulus variations (which are indeed larger, around 30–35%), but the trend is clearly conserved so that it can be concluded that the monolayer resistance to pure bending increases with the sugar concentration.

References

Branca C, Magazù S, Migliardo F, Migliardo P (2002) Destructuring effect of trehalose on the tetrahedral network of water: a Raman and neutron diffraction comparison. Physica A 304:314–318

Cevc G (1991) Polymorphism of the bilayer membranes in the ordered phase and the molecular origin of the lipid pretransition and rippled lamellae. Biochim Biophys Acta 1062:59–69

Chen Z, Rand RP (1998) Comparative study of the effects of several *n*-alkanes on phospholipid hexagonal phases. Biophys J 74:944–952

Collins KD, Washabaugh MW (1985) The Hofmeister effect and the behaviour of water at interfaces. Q Rev Biophys 18:323–422

Cordone L, Galajda P, Vitrano E, Gassmann A, Ostermann A, Parak F (1998) A reduction of protein specific motions in coligated myoglobin embedded in trehalose glass. Eur Biophys J 27:173–176

Cottone G, Ciccotti G, Cordone L (2002) Protein-trehalose-water structures in trehalose coated carboxy-myoglobin. J Chem Phys 117:9862–9866

Crowe JH, Crowe LM (1988) Trehalose and dry dipalmitoyl phosphatidylcholine revisited. Biochim Biophys Acta 946:193–201

Crowe JH, Crowe LM, Chapman D (1984) Preservation of membranes in anhydrobiotic organisms: the role of trehalose. Science 223:701–703

Crowe LM (2002) Lessons from nature: the role of sugars in anhydrobiosis. Comp Biochem Physiol A 131:505–513

Crowe LM, Crowe JH, Carpenter JF, Wistrom CA (1987) Stabilization of dry phospholipid bilayers and proteins by sugars. Biochem J 242:1–10

Evans E, Needham D (1987) Physical properties of surfactant bilayer membranes: thermal transitions, elasticity, rigidity, cohesion and colloidal interactions. J Phys Chem 91:4219–4228

Fuller N, Rand RP (2001) The influence of lysolipids on the spontaneous curvature and bending elasticity of phospholipid membranes. Biophys J 81:243–254

Gawrish K, Parsegian VA, Hajduk DA, Tate MW, Gruner SM, Fuller NL, Rand RP (1992) Energetics of a hexagonal-kamellar-hexagonal phase transition sequence in dioleoylphosphatidylethanolamine membranes. Biochemistry 31:2856–2864

Harper PE, Mannock DA, Lewis RNAH, McElhaney RN, Gruner SM (2001) X-ray diffraction structures of some phosphatidylethanolamine lamellar and inverted hexagonal phases. Biophys J 81:2693–2706

Heerklotz H, Seelig J (2002) Application of pressure perturbation calorimetry to lipid bilayers. Biophis J 82:1445–1452

Helfrich W (1973) Elastic properties of lipid bilayers: theory and possible experiments. Z Naturforsch C 28:693–703

Koynova R, Caffrey M (1994) Phases and phase transitions of the hydrated phosphatidylethanolamines. Chem Phys Lipids 62:253–262

Koynova RD, Tenchov BG, Quinn PJ (1989) Sugars favor formation of hexagonal phase at the expense of the lamellar liquid-crystalline phase in hydrated phosphatidylethanolamines. Biochim Biophys Acta 980:377–380

Koynova R, Brankov J, Tenchov B (1997) Modulation of the lipid phase behaviour by kosmotropic and chaotropic solutes. Eur Biophys J 25:261–275

Kozlov MM, Winterhalter M (1991) Elastic moduli for strongly curved monolayers. Position of the neutral surface. J Phys II (France) 1:1077–1084

Kozlov MM, Leikin S, Rand RP (1994) Bending, hydration and interstitial energies quantitatively account for the hexagonal-lamellar-hexagonal reentrant phase transition in dioleoyl phosphatidyl ethanolamine. Biophys J 67:1603–1611

Leikin S, Kozlov MM, Fuller NL, Rand RP (1996) Measured effects of diacylglycerol on structural and elastic properties of phospholipid membranes. Biophys J 71:2623–2632

Librizzi FC, Viappiani C, Abbruzzetti S, Cordone L (2002) Residual water modulates the dynamics of the protein and of the external matrix in "trehalose coated" MbCO: an infrared and flash photolysis study. J Chem Phys 116:1193–1200

Lide DR (1996) Handbook of chemistry and physics, 77th edn. CRC, Boca Raton

Luzzati V (1968) X-ray diffraction studies of lipid-water systems. In: Chapman D (ed) Biological Membranes, vol 1, chap 3. Academic Press, London, pp 71–123

Mariani P, Luzzati V, Delacroix H (1988) Cubic phases of lipid-containing systems. Structure analysis and biological implications. J Mol Biol 204:165–189

Mariani P, Rustichelli F, Saturni L, Cordone L (1999) Stabilization of the monoolein *Pn3m* cubic structure on trehalose glasses. Eur Biophys J 28:294–301

Parsegian VA, Rand RP, Fuller NL, Rau DC (1986) Osmotic stress for the direct measurement of intermolecular forces. Methods Enzymol 127:400–416

Perry RN, Clarke AJ, Hennessy J (1980) The influence of osmotic pressure on the hatching of *Heterodera schachtii*. Rev Nematol 3(1):3–9

Rand RP, Fuller NL (1994) Structural dimensions and their changes in a reentrant hexagonal-lamellar transition of phospholipids. Biophys J 66:2127–2138

Rand RP, Fuller NL, Parsegian VA, Rau DC (1988) Variation in hydration forces between neutral phospholipid bilayer: evidence for hydration attraction. Biochemistry 27:7711–22

Rand RP, Fuller NL, Gruner SM, Parsegian VA (1990) Membrane curvature, lipid segregation and structural transitions for phospholipids under dual-solvent stress. Biochemistry 29:76–87

Rappolt M, Hickel A, Bringezu F, Lohner K (2003) Mechanism of the lamellar/inverse hexagonal phase transition examined by high resolution X-ray diffraction. Biophys J 84:3111–3122

Rau DC, Parsegian VA (1992) Direct measurement of the intermolecular forces between counterion-condensed DNA double helices. Evidence for long range attractive hydration forces. Biophys J 61:246–259

Rau DC, Lee B, Parsegian VA (1984) Measurement of the repulsive force between polyelectrolyte molecules in ionic solution: hydration forces between parallel DNA double helices. Proc Natl Acad Sci USA 81:2821–2825

Rector D, Jiang J, Berg MA, Fayer MD (2001) Effects of solvent viscosity on protein dynamics: infrared vibrational echo experiments and theory. J Phys Chem B 105:1081–1092

Salmon A, Dodd W, Williams GD, Beach JM, Brown MF (1987) Configurational statistics of acyl chains in polyunsaturated lipid bilayers from H-2 NMR. J Am Chem Soc 109:2600–2609

Sanderson PW, Lis LJ, Quinn PJ, Williams WP (1991) The Hofmeister effect in relation to membrane lipid phase stability. Biochim Biophys Acta 1067:43–50

Sankaram MB, Thompson TE (1992) Deuterium magnetic resonance study of phase equilibria and membrane thickness in binary phospholipid mixed bilayers. Biochemistry 31:8258–8268

Saturni L, Rustichelli F, Di Gregorio GM, Cordone L, Mariani P (2001) Sugar-induced stabilization of the monoolein *Pn*3*m* bicontinuous cubic phase during dehydration. Phys Rev E 64:0409021–4

Seelig J, Seelig A (1974) Deuterium magnetic resonance studies of phospholipid bilayers. Biochem Biophys Res Commun 57:406–411

Shalaev EY, Steponkus PL (2001) Phase behavior and glass transition of 1,2-dioleoylphosphatidylethanolamine (DOPE) dehydrated in the presence of sucrose. Biochim Biophys Acta 1514:100–116

Szule JA, Rand RP (2003) The effects of gramicidin on the structure of phospholipid assemblies. Biophys J 85:1702–1712

Takahashi H, Ohmae H, Hatta I (1997) Trehalose-induced destabilization of interdigitated gel phase in dihexadecylphosphatidylcholine. Biophys J 73:3030–3038

Templer RH, Turner DC, Harper P, Seddon JM (1995) Corrections to some models of the curvature elastic energy of inverse bicontinuous cubic phases. J Phys II (France) 5:1053–1065

Templer RH, Seddon JM, Warrender NA, Syrykh A, Huang Z, Winter R, Erbes J (1998) Inverse bicontinuous cubic phases in 2:1 fatty acid/phosphatidylcholine mixtures. The effects of chain length, hydration, and temperature. J Phys Chem 102:7251–7261

Tenchov B, Koynova R, Rapp G (2001) New ordered metastable phases between the gel and subgel phases in hydrated phospholipids. Biophys J 80:1873–1890

Tsonev LI, Tihova MG, Brain APR, Yu Z-W, Quinn PJ (1994) The effect of cryoprotective sugar, trehalose, on the phase behaviour of mixed dispersions of dioleoyl derivatives of phosphatidylethanolamine and phosphatidylcholine. Liq Cryst 17:717–728

Turner DC, Gruner SM (1992) X-ray diffraction reconstruction of the inverted hexagonal (H_{II}) phase in lipid-water systems. Biochemistry 31:1340–1355

Vacklin H, Khoo BJ, Madan KH, Seddon JM, Templer RH (2000) The bending elasticity of 1-monoolein upon relief of packing stress. Langmuir 16:4741–4748

Wistrom CA, Rand RP, Growe LM, Spargo BJ, Crowe JH (1989) Direct transition of dioleoylphosphatidylethanolamine from lamellar gel to inverted hexagonal phase caused by trehalose. Biochim Biophys Acta 984:238–242

Zhang J, Steponkus PL (1996) Proposed mechanism for depression of the liquid-crystalline-to-gel phase transition temperature of phospholipids in dehydrated sugar-phospholipids mixtures. Cryobiology 33:21A